Radiation Measurements xxx (2009) 1–5

Contents lists available at ScienceDirect

Radiation Measurements

journal homepage: www.elsevier.com/locate/radmeas

Lunar soil as shielding against space radiation

J. Miller [a,*], L. Taylor [b], C. Zeitlin [c], L. Heilbronn [d], S. Guetersloh [e], M. DiGiuseppe [f], Y. Iwata [g], T. Murakami [g]

[a] Lawrence Berkeley National Laboratory, MS 83R0101, 1 Cyclotron Road, Berkeley, CA 94720, USA
[b] Planetary Geosciences Institute, Department of Earth and Planetary Sciences, The University of Tennessee, Knoxville, TN 37996, USA
[c] Southwest Research Institute, Boulder, CO 80302, USA
[d] Department of Nuclear Engineering, The University of Tennessee, Knoxville, TN 37996, USA
[e] Department of Nuclear Engineering, Texas A&M University, College Station, TX 77843, USA
[f] Northrop Grumman Corporation, Bethpage, NY 11714, USA
[g] National Institute of Radiological Sciences, Chiba 263-8555, Japan

A R T I C L E I N F O

Article history:
Received 6 August 2008
Accepted 28 January 2009

Keywords:
Lunar soil
Lunar regolith
Space radiation shielding
Galactic cosmic radiation (GCR)
Solar particle event (SPE)

A B S T R A C T

We have measured the radiation transport and dose reduction properties of lunar soil with respect to selected heavy ion beams with charges and energies comparable to some components of the galactic cosmic radiation (GCR), using soil samples returned by the Apollo missions and several types of synthetic soil glasses and lunar soil simulants. The suitability for shielding studies of synthetic soil and soil simulants as surrogates for lunar soil was established, and the energy deposition as a function of depth for a particular heavy ion beam passing through a new type of lunar highland simulant was measured. A fragmentation and energy loss model was used to extend the results over a range of heavy ion charges and energies, including protons at solar particle event (SPE) energies. The measurements and model calculations indicate that a modest amount of lunar soil affords substantial protection against primary GCR nuclei and SPE, with only modest residual dose from surviving charged fragments of the heavy beams.

1. Introduction

Exposure to space radiation may be a limiting factor in future manned lunar missions. In contrast to the brief stays by the Apollo astronauts, in the coming decades, humans will remain on the lunar surface for weeks and eventually months at a time. Chronic exposure to highly ionizing ions in the galactic cosmic radiation (GCR) and sporadic acute exposures to protons emitted in solar proton events (SPE) are health hazards that can be mitigated in part by radiation shielding. The spacecraft, spacesuits and rovers will provide only modest shielding, and the expense of transporting material to the moon will allow for little if any supplemental shielding material. An alternative is the essentially unlimited supply of lunar soil,[1] if ways can be found to effectively use it. We have undertaken a study of the radiation transport and dose reduction properties of lunar soil, using samples returned by the Apollo missions and several types of synthetic soil glasses and lunar soil simulants, with the objectives of evaluating soil as potential shielding and of man-made soil as a surrogate for use in ground-based studies. Reliable synthetics and simulants are needed due to the extreme scarcity of Apollo soil samples. Beams of protons and heavier charged particles at energies comparable to the most biologically damaging components of the GCR are available at a few accelerator facilities, including the Heavy Ion Medical Accelerator in Chiba (HIMAC) at the Japanese National Institute of Radiological Sciences, at which the data reported here were obtained.

2. Materials and methods

The Apollo soil samples, synthetic glasses with soil compositions, and man-made simulants (from terrestrial rocks) that were used in the radiation experiments performed during this study are listed in Tables 1 and 2. According to lunar scientific usage, lunar regolith is all the broken rock materials that cover the Moon; soil is the <1 cm portion of this regolith (McKay et al., 1991).

* Corresponding author. Tel.: +1 510 486 7130; fax: +1 510 486 6880.
E-mail address: miller@lbl.gov (J. Miller).

[1] Here we make the distinction between lunar soil and lunar regolith. While the terms are often used interchangeably, regolith is defined to include boulders and larger materials, in addition to the smaller sizes. The materials used in this study are all actual Apollo, synthetic or simulated lunar soil. The simulants were made to duplicate some particular aspect of the lunar soils – *e.g.*, the grain-size distribution, composition and/or glass content.

1350-4487/$ – see front matter © 2009 Elsevier Ltd. All rights reserved.
doi:10.1016/j.radmeas.2009.01.010

Table 1
Soil samples, synthetic soils and simulants used in this study.

Sample	Source and description
L-10084	Apollo 11 – high-Ti mare soil
A-61141	Apollo 16 – highland soil
L-61501	Apollo 16 – highland soil
L-62241	Apollo 16 – highland soil
A-64501	Apollo 16 – highland soil
A-70051	Apollo 17 – high-Ti mare soil
S-15041	Synthetic Apollo 15 soil; low-Ti mare
S-67461	Synthetic Apollo 16 – highland soil
S-70051	Synthetic Apollo 17 – high-Ti mare soil
JSC-1A	Johnson Space Center Lunar Simulant 1A; 50–50 mare + highland soil
JSC-1AF	Johnson Space Center Simulant, fused to 100% glass
MLS-1A	Minnesota Lunar Simulant 1A; composition similar to L-10084
NU-LHT-1	Lunar Highland Soil Simulant; USGS Denver
MLS-2	Minnesota Lunar Simulant 2; highland anorthosite ground
“Claudia”	Lunar Highland Simulant; highland anorthosite ground
“Hap”	Lunar Highland Simulant; highland anorthosite ground

2.1. Apollo lunar soils and synthetic lunar soils

The lunar soils were chosen from soils that have been well-characterized (Pieters et al., 2000; Taylor et al., 2000, 2001a, b) and are representative of the different terrains on the Moon. The mare regions (dark regions of the lunar surface) are represented by the high-Ti soils at the Apollo 11 and 17 landing sites. Highland soils (light-colored surface regions) are represented by four Apollo 16 soils, which are high in Ca-plagioclase feldspar, low in Fe–Mg minerals, and have different degrees of maturity – *i.e.*, times of exposure at the lunar surface. Glasses were synthesized from silica gels mixed with other cation components, and resulted in glasses with compositions similar to those of soils collected by the Apollo 15, 16 and 17 Missions.

2.2. Lunar soil simulants

Due to the precious nature of the Apollo lunar samples, it is not always possible to use the Apollo samples for experiments that are being performed in preparation for a manned lunar outpost. Lunar soil simulant, JSC-1, was made in 1993 by crushing a welded volcanic tuff quarried north of Flagstaff, AZ. It contained about 50% glass, similar to lunar soils. This basalt was ground and sized to be approximately the same as average lunar soil, had engineering (geotechnical) properties similar to those of lunar soil, but had a composition that was unrepresentative of 95% of the lunar soils – it was, approximately half mare and half highland in composition. The original 20 ton of JSC-1 were distributed free of charge to the public by NASA. In 2007, a second batch of this same lunar soil simulant was made and denoted JSC-1A.

Shortly after the return of Apollo 11 in 1969, a hi-Ti diabase from Duluth, Minnesota was ground up to produce the Minnesota Lunar Simulant, MLS-1 (Weiblen et al., 1990). MLS-1 has a composition close to the hi-Ti Apollo 11 soil 10084 (Goldich, 1971). The same group also ground up anorthosite from the Duluth Gabbro Complex and made MLS-2, a lunar highland soil simulant. In 2007, the USGS in Denver produced a lunar highland soil simulant, NU-LHT-1, which has abundant glass, plagioclase, and a bulk composition similar to typical highland soil (*i.e.*, 4–5 wt% FeO). Two other highland anorthosite simulants “Claudia” and “Hap” were produced for this study. These samples were collected at Bowles Butte, Idaho, and the Stillwater Complex, Montana, respectively, and are composed mainly of high-Ca-plagioclase feldspars. The compositions of the samples used in these radiation experiments are given in Table 2.

2.3. Radiation experiments

The radiation measurements were made at HIMAC in two phases. A pilot study in February 2007 explored the variation of shielding effectiveness for soil from different sites on the Moon, and the suitability for shielding studies of synthetic soil glasses and soil simulants as a surrogate for lunar soil. In the second phase (January 2008), the average energy depositions in silicon solid state detectors as a function of depth—analogous to a depth–dose distribution—were measured for a particular beam passing through one type of simulant. As explained elsewhere (Zeitlin et al., 2006), the average energy deposition can be used as a measure of the shielding effectiveness of various materials. There is considerable dependence of the results on the beam ion and energy (Guetersloh et al., 2006), and it has been shown that the best proxies for the heavy ion component of the GCR are high energy beams of oxygen or heavier species. The present study has been carried out with beam energies that are lower than optimal for purposes of simulating the GCR. Nonetheless, significant results have been obtained.

Table 2
Chemical compositions of the soil samples used in the radiation experiments.

Type	L-10084	L-61141	L-61501	L-62241	L-64501	L-70051	S-15041	S-67461	S-70051	JSC-1A	JSC-1A Glass	MLS-1	NU-LHT-1	MLS-2	Claudia	Hap
	Mare	Hi-lnd	Hi-lnd	Hi-lnd	Hi-lnd	Mare	Mare	Hi-lnd	Mare	M + H	M + H	Mare	Hi-lnd	Hi-lnd	Hi-lnd	Hi-lnd
Source	Apollo	Apollo	Apollo	Apollo	Apollo	Apollo	Synth-	Synth-	Synth-	Earth	Earth	Earth	Earth	Earth	Earth	Earth
SiO_2	41.0	45.2	44.66	44.65	46.5	42.2	46.5	43.1	41.0	46.2	46.2	42.8	44.2	48.3	62.0	48.8
TiO_2	7.3	0.58	0.56	0.56	0.53	5.09	1.80	0.40	4.80	1.85	1.85	6.77	0.32	0.03	21.5	30.1
Al_2O_3	12.8	26.4	26.5	27.0	27.4	15.7	13.6	28.7	17.2	17.1	17.1	12.1	27.9	32.4	0.4	2.3
Cr_2O_3	0.31	0.13											0.17			
FeO	16.2	5.29	5.31	5.49	4.16	12.4	15.4	5.00	13.5	11.2	11.2	16.3	4.22	0.45	1.2	0.4
MnO	0.22	0.70	0.07	0.70		0.15				0.19	0.19	0.22	0.09			
MgO	9.20	6.10	6.08	5.84	4.27	10.3	10.4	4.10	10.7	6.87	6.87	6.19	7.92	0.15	8.3	14.9
CaO	12.4	15.32	15.33	15.95	16.6	11.5	10.3	17.0	11.9	9.43	9.43	11.1	12.5	16.0	5.7	2.6
Na_2O	0.38	0.52	0.41	0.44	0.47	0.24				3.33	3.33	2.22	1.32	2.42	0.4	0.2
K_2O	0.15	0.14	0.11	0.13	0.11	0.07				0.85	0.85	0.20	0.09	0.06		
P_2O_5		0.12	0.11	0.10						0.62	0.62	0.04				
LOI										0.70	0.70	0.85		0.62	0.45	0.48
Total	99.96	100.50	99.14	100.86	100.14	97.65	98.0	98.3	99.1	98.34	98.34	98.79	98.73	100.43	99.95	99.78

LOI: Loss on Ignition.
Table 1 lists the provenance of these soils. The data for the Apollo soils, except for Apollo 17 soil 70051 (Hill et al., 2007), are from the Handbook of Lunar Soils, compiled by Morris et al. (1983). The synthetic simulants were prepared for and all of the “Earth” samples were collected and analyzed during this study.

Please cite this article in press as: Miller, J., et al., Lunar soil as shielding against space radiation, Radiation Measurements (2009), doi:10.1016/j.radmeas.2009.01.010

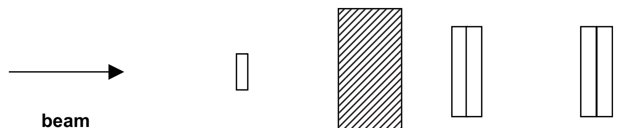

Fig. 1. Detector schematic (Not to scale). All detectors except TR are lithium-drifted silicon. TR dimensions are 300 µm thick × 4 mm active radius, and the downstream detectors are a mix of 1 mm thick × 2 cm radius; 3 mm thick × 1.1 cm radius; and 5 mm thick × 2 cm active radius.

2.4. Phase I

Samples of Apollo soil, synthetic soil glasses and soil simulant were placed in a beam of 400 MeV/nucleon ^{10}B ions. Charged fragments and beam ions that survived traversal of the target passed through a stack of silicon detectors centered on the beam axis downstream of the target, and the energy deposited in each detector was recorded. The detector setup (Fig. 1) was similar to that used in previous measurements by our group. (Typically we use a mix of detector sizes according to the beam and target (see, *e.g.*, Zeitlin et al., 2007).) The beam spot at TR was an ellipse with major and minor axes less than 5 mm. Offline analysis yielded energy deposition (ΔE) spectra, from which the percent dose reduction per incident beam ion normalized to unit material depth was calculated by methods described in detail in Zeitlin et al. (2006). The data for each target were compared to one another and to results for standard shielding materials.

Energy deposited in one or more silicon detectors downstream of the target was converted to a pulse height and digitized by the data acquisition electronics, and in the first-pass data processing the pulse heights were converted to ΔE values. In subsequent analysis steps, sub-samples of well-measured events were obtained by requiring that one (and only one) primary beam ion was seen in the detector upstream of the target, and that the ΔE values recorded in the detector pair closest to the target exit were well-correlated with one another. For analysis of the Phase I data, we used PSD1, the first silicon detector pair after the target, which subtended an acceptance cone of half-angle 9.5° centered on the beam axis.

Following the method described in Zeitlin et al. (2006), the dose reduction per incident beam particle, δD, behind shielding was calculated to be

$$\delta D = 1 - \left(\frac{\Delta E_{\text{avg-in}}}{\Delta E_{\text{avg-out}}}\right)$$

where "in" and "out" refer to measurements with and without a target, respectively, and "avg" is an "event-averaged" rather than "track-averaged" quantity.[2]

The dose reduction was then normalized to the target's areal density, $\rho\Delta x$, in g cm^{-2} to give the dose reduction per unit areal density, δD_n, in (g cm^{-2})$^{-1}$.

2.5. Phase II

In the second round of experiments, a number of depths of lunar highland soil simulant NU-LHT-1, were placed in a beam of 290 MeV/nucleon ^{10}B ions. NU-LHT-1 was formulated to simulate the expected highland soil composition at the lunar south pole, a likely location for future human outposts. The detector setup and data analysis were similar to those used in Phase I. Data were obtained with soil depths between 0 and 30 g cm^{-2} with an average density of 1.71 g cm^{-3}.[3]

Table 3
Dose reduction.

Target	Depth (g cm^{-2})	δD	δD_n (g cm^{-2})$^{-1}$
Apollo 16, 61501	7.54	0.071	0.009
Apollo 16, 62241	7.52	0.066	0.009
Apollo 16, 64501	5.97	0.044	0.007
Apollo 16, 61141	12.33	0.103	0.008
Apollo 11, 10084	6.67	0.056	0.008
Apollo 17, 70051	11.68	0.111	0.010
Simulant JSC-1A	12.89	0.116	0.009
Simulant JSC-1AF	12.65	0.115	0.009
Simulant MLS-1A	12.37	0.110	0.009
Simulant MLS-2	12.37	0.121	0.010
Simulant "Claudia"	12.53	0.122	0.010
Simulant "Hap"	12.48	0.114	0.009
Synthetic 67461	12.01	0.103	0.009
Synthetic 15041	12.54	0.106	0.008
Synthetic 70051	12.49	0.108	0.009
Aluminum	5.4	0.054	0.010
Graphite	7.2	0.111	0.015
Polyethylene	4.81	0.095	0.020

3. Results and discussion

3.1. Phase I

The δD_n values calculated from the Phase I data are tabulated in Table 3, along with δD_n for three other materials of interest: aluminum, used in conventional spacecraft hulls, polyethylene (CH_2) a common tissue surrogate, and graphite, a light and strong structural material with potential for use in spacecraft. The results are presented graphically in Fig. 2. In the figure the soil results are averaged and a calculated dose reduction for lead is included. We note that δD_n takes into account the weight penalty of importing shielding, *e.g.*, 1 cm lead reduces dose by almost the same percentage as 1 cm polyethylene, but with a much greater mass penalty. The percent dose reduction per unit areal density of the soil, synthetic soil, and soil simulant varied between 0.7% and 1.0%, comparable to that of aluminum and approximately half that of polyethylene. Observed differences in normalized dose reduction between the Apollo soil samples, the synthetic soil glasses and the lunar soil simulants were small.

For this beam, the average percent dose reduction over all soil samples is 0.8%, compared to 0.9% for aluminum. This similarity is not unexpected: for Apollo sample A70051, for example, the weighted average mass number of the constituents is 26.3 and the weighted average atomic number is 12.85, compared to nominal A and Z for aluminum of 27 and 13, respectively. In other words, per unit areal density, lunar soil is only slightly less effective than aluminum, and only about half as effective as polyethylene at reducing dose for this particular ion and energy. Of course, soil has the great advantage of being available *in situ* on the Moon.

3.2. Phase II

The Phase I results established that for one heavy ion beam at a single energy in the midrange of the GCR, Apollo lunar soil from

[2] As discussed in Zeitlin et al. (2006), we make two assumptions: (1) that the total dose is dominated by particles emitted within a narrow cone along the beam axis and (2) that the dose per beam particle is dominated by a single particle, even though for each interacting beam particle more than one particle may be emitted, hence the reference to "event-average" rather than "track-average" energy loss.

[3] Simply poured lunar soil has a density of approximately 1 g cm^{-3} (Carrier et al., 1991). The simulant was packed to an average density of 1.41 g cm^{-3}, but the density of the samples was subsequently measured to be 1.71 g cm^{-3} due to settling during shipment.

Please cite this article in press as: Miller, J., et al., Lunar soil as shielding against space radiation, Radiation Measurements (2009), doi:10.1016/j.radmeas.2009.01.010

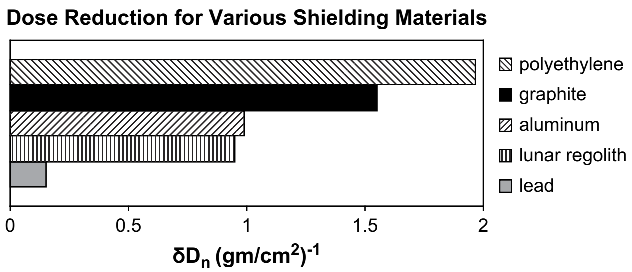

Fig. 2. Percent dose reduction δD_n per unit areal density (in g cm^{-2}) for lunar regolith compared to polyethylene, graphite, aluminum and lead. (The dose reduction for lunar regolith is an average over all samples tested.)

several different sites, synthetic soil glasses, and lunar soil simulants are approximately equally effective per unit areal density in reducing radiation dose. Further, the data show that soil is quite comparable to aluminum in its shielding properties. In Phase II, we measured the energy deposited in silicon detectors per incident beam ion as a function of depth in a single soil simulant (NU-LHT-1) and for a beam of 290 MeV/nucleon ^{10}B ions. An energy spectrum was measured with no target and at eight depths of soil between 7.5 and 30 g cm^{-2}.

A heavy charged particle beam passing through a thick target is modified by electromagnetic and nuclear interactions with the target atoms. Electromagnetic interactions with the atomic electrons tend to slow the beam ions, so that they are more ionizing at the target exit than they were at the target entrance. Nuclear interactions break the beam ions into more lightly charged and therefore, less ionizing (but longer range) fragments. The interplay of these effects as a function of depth produces the characteristic ionization "Bragg curve". As shown previously (Zeitlin et al., 1998; Guetersloh et al., 2006) with a ^{12}C beam at the same energy, over the first few g cm^{-2} of material, the effects approximately balance each other, and the average energy deposition per incident beam ion is close to constant. At greater depths, the slower and more highly ionizing beam particles begin to dominate and the average energy deposition rises rapidly to the Bragg peak. Beyond the Bragg peak, only lightly ionizing fragments remain, and the average energy deposition per incident beam ion decreases rapidly. This is illustrated in Figs. 3 and 4. With no target (Fig. 3a), the spectrum is dominated by the beam ions, only slightly modified by passage through a few cm of air, the 300 μm trigger silicon detector, and the 3 mm silicon detector. After passing through 16.4 g cm^{-2} soil (Fig. 3b), the beam peak is shifted to higher energy deposition, and there is noticeable fragmentation, but this is compensated by the increased ionization of the surviving beam ions, and the average energy deposition is almost the same as the value with no soil. After 22 g cm^{-2} (Fig. 3c) of lunar soil simulant, the primary ions are approaching their peak ionization, and after 26.6 g cm^{-2} (Fig. 3d), the primary beam ions have all stopped, only lightly ionizing fragments remain, and the dose approaches a minimum. The solid line in Fig. 4 summarizes the results. Note that the beam is almost completely attenuated after 25 g cm^{-2} of soil (approximately 20 cm assuming a density of approximately 1.4 g cm^{-3}).

4. Model comparison

The data reported here were taken with a single heavy ion at two similar energies. The GCR heavy ion flux, when weighted by dose, has significant components for elements from hydrogen through iron ($Z=26$, $A=56$) over several orders of magnitude in energy from 10^2 to at least 10^4 MeV/nucleon. A proper survey would sample several data points over these ranges, but such a study must await the availability of suitable accelerator beams. In the meantime, we have made use here of a model (Zeitlin et al., 1996) that has been shown (Miller et al., 2003; Guetersloh et al., 2006) to reproduce with good accuracy the energy deposition of a number of different heavy ion beams in thick targets. The model calculation for these data is shown as the dashed line in Fig. 4. There is good agreement between the data and the model. We then used the model to estimate the thickness of soil needed to stop several representative components of the GCR, and the energy deposited by the residual fragments. The results are shown in Table 4. The rightmost column is the ratio of the energy deposited by fragments downstream of the stopping peak (at a point analogous to the 25 g cm^{-2} point in Fig. 4) to the peak energy deposition at the end

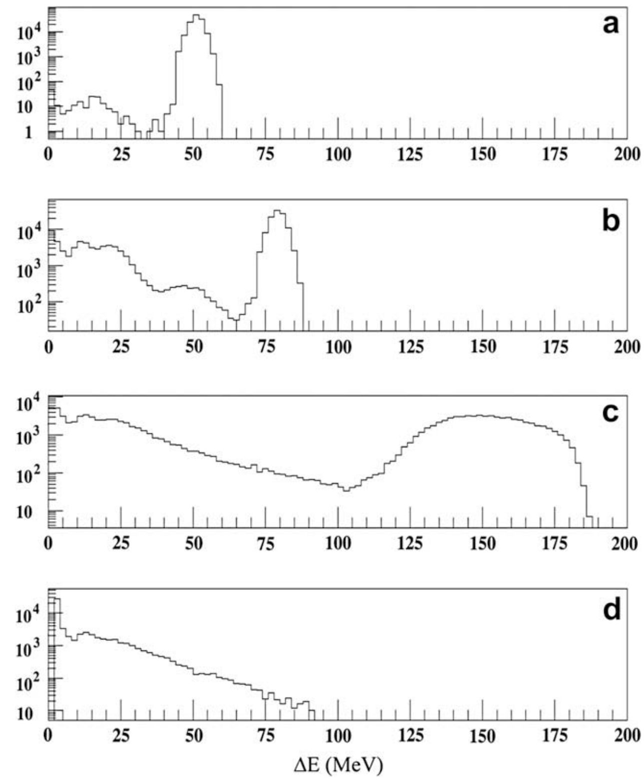

Fig. 3. Energy lost by a 290 MeV/nucleon ^{10}B beam and its charged fragmentation products in a 3 mm silicon detector after passing through (a) 0 g cm^{-2}, (b) 16.4 g cm^{-2}, (c) 22 g cm^{-2}, and (d) 26.6 g cm^{-2} lunar regolith simulant.

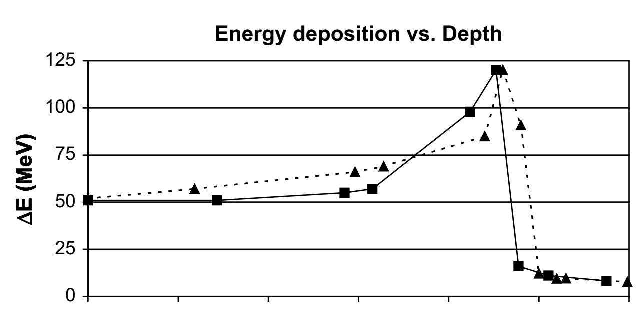

Fig. 4. Energy deposition in a 3 mm silicon detector for a 290 MeV/nucleon ^{10}B beam after passing through lunar highland regolith simulant.

Table 4
Range and residual energy deposition by charged fragments.

Beam	T_{beam} (MeV/u)	Range (cm)	$\Delta E_{residual}/\Delta E_{peak}$
p	50	2.0	–
	100	7.1	–
	200	23.1	–
	300	46.2	–
	500	107.4	–
^{4}He	50	2.0	0.0005
	100	7.1	0.004
	300	46.2	0.006
^{10}B	290	17.7	0.10
^{12}C	100	2.3	0.03
	500	35.4	0.07
	1000	99.3	0.06
^{28}Si	100	1.0	0.01
	500	15.0	0.09
	1000	42.2	0.14
^{56}Fe	100	0.6	0.0001
	500	8.8	0.10
	1000	24.5	0.20

of the particle's range in soil, which gives an indication of the residual dose after the primary ion stops in the soil.

From the model calculation, we find that less than a half-meter of soil (compacted to a density of 1.4 g cm^{-3}) is sufficient in almost every case to stop primary GCR ions, and that the remaining dose from charged fragments is in all but two cases less than 10% of the dose in the Bragg peak. (The exceptions being ^{28}Si and ^{56}Fe at 1000 MeV/nucleon, heavy ions for which one expects there to be a relatively high number of high energy heavy fragments produced in the soil.) The same is true for protons up to 300 MeV, which is sufficient for all but the hardest SPE spectrum and energetic GCR protons.

5. Conclusion

We have studied the transport properties of lunar soil, synthetic soil glasses, and soil simulants with respect to protons and heavier nuclei representative of the radiation field at the lunar surface. The utility of synthetic soil glasses and simulant as surrogates for actual soil in radiation transport studies has been established by comparing the dose reduction across materials. A new type of lunar highland simulant was then used to take a depth–dose curve for one species of heavy ion at a single energy, and a fragmentation and energy loss model was used to extend the results over a range of nuclear charges and energies.

The measurements and model calculations indicate that a fairly small amount of soil, slightly compacted from 1 to 1.4 g cm^{-3}—46 cm or less—affords substantial protection against primary GCR nuclei and SPE protons, with only modest residual dose from surviving charged fragments of the heavy beams. It is important to note that we have not accounted for the dose from neutrons in either the data or the calculations. The dose from neutrons created by heavy ions and low energy protons can be estimated from thick target data [see, *e.g.*, (Kurosawa et al., 1999)], but additional measurements and modeling efforts would be helpful in this regard.

Studies of this type will help mission planners determine the efficacy of lunar soil as shielding against GCR heavy ions for astronauts on future lunar missions. The results suggest that use of *in situ* resources on the lunar surface holds promise for radiation protection, with modest amounts of lunar soil providing substantial protection against both GCR and SPE particles.

Acknowledgements

We thank the Lunar Sample Curator and CAPTEM for providing the Apollo samples for these studies. This work was supported in part by the Northrop Grumman Corporation, by the RESOLVE program at NASA-Johnson Space Center, by the Planetary Geosciences Institute at the University of Tennessee, and at LBNL under NASA Contracts numbers L14230C, H31910D and H34854D, through the US Department of Energy under Contract No. DE-AC02-05CH11231.

References

Carrier III, W.D., Olhoeft, G.R., Mendell, W., 1991. Physical properties of the lunar surface. In: Heiken, G.H., Vaniman, D.T., French, B.M. (Eds.), Lunar Sourcebook. Cambridge University Press, Cambridge (Chapter 9).
Goldich, S.S., 1971. Lunar and terrestrial ilmenite basalt. Science 171, 1245–1246.
Guetersloh, S.B., Zeitlin, C., Heilbronn, L., Miller, J., Komiyama, T., Fukumura, A., Iwata, Y., Murakami, T., Bhattacharya, M., 2006. Polyethylene as a radiation shielding standard in simulated cosmic-ray environments. Nucl. Instrum. Methods Phys. Res. B 252, 319–332.
Hill, E., Mellin, M.J., Deane, B., Liu, Y., Taylor, L.A., 2007. Apollo sample 70051 and high- and low-Ti lunar soul simulants MLS-1A and JSC-1A: implications for future lunar exploration. J. Geophys. Res. 112, E02006, doi:10.1029/2006JE002767.
Kurosawa, T., Nakao, N., Nakamura, T., Uwamino, Y., Shibata, T., Nakanishi, N., Fukumura, A., Murakami, K., 1999. Measurements of secondary neutrons produced from thick targets bombarded by high-energy helium and carbon ions. Nucl. Sci. Eng. 132, 30–57.
McKay, D.S., Heiken, G., Basu, A., Blanford, G., Simon, S., Reedy, R., French, B.M., Papike, J., 1991. The lunar regolith. In: Heiken, G.H., Vaniman, D.T., French, B.M. (Eds.), Lunar Sourcebook. Cambridge University Press, Cambridge (Chapter 6).
Miller, J., Zeitlin, C., Cucinotta, F.A., Heilbronn, L., Stephens, D., Wilson, J.W., 2003. Benchmark studies of the effectiveness of structural and internal materials as radiation shielding for the international space station. Radiat. Res. 159, 381–390.
Morris, R.V., Score, R., Dardano, C., Heiken, G., 1983. Handbook of Lunar Soils – Part 1: Apollo, vols. 11–15, pp. 1–422.
Morris, R.V., Score, R., Dardano, C., Heiken, G., 1983. Handbook of Lunar Soils – Part 2: Apollo, vols. 16–17, pp. 423–914.
Pieters, C.M., Taylor, L.A., Noble, S.K., Keller, L.P., Hapke, B., Morris, R.V., Allen, C.C., McKay, D.S., Wentworth, S., 2000. Space weathering on airless bodies: resolving a mystery with lunar samples. Meteorit. Planet. Sci. 35, 1101–1107.
Taylor, L.A., Pieters, C., Keller, L.P., Morris, R.V., McKay, D.S., Patchen, A., Wentworth, S., 2000. Space weathering of lunar mare soils: new understanding of the effects of reflectance spectroscopy. In: Space 2000. American Society of Civil Engineers, pp. 703–711.
Taylor, L.A., Pieters, C., Keller, L.P., Morris, R.V., McKay, D.S., Patchen, A., Wentworth, S., 2001a. The effects of space weathering on Apollo 17 mare soils: petrographic and chemical characterization. Meteorit. Planet. Sci. 36, 285–299.
Taylor, L.A., Pieters, C.M., Keller, L.P., Morris, R.V., McKay, D.S., 2001b. Lunar mare soils: space weathering and the major effects of surface-correlated nanophase Fe. J. Geophys. Lett. 106, 27,985–27,999.
Weiblen, P.W., Murawa, M.J., Reid, K.J., 1990. Preparation of simulants for lunar surface materials. In: Engineering, Construction and Operations in Space II. American Society of Civil Engineers, New York, pp. 428–435.
Zeitlin, C., Heilbronn, L., Miller, J., Schimmerling, W., Townsend, L.W., Tripathi, R.K., Wilson, J.W., 1996. The fragmentation of 510 MeV/nucleon iron-56 in polyethylene. II. Comparisons between data and a model. Radiat. Res. 145, 666–672.
Zeitlin, C., Heilbronn, L., Miller, J., 1998. Detailed characterization of the 1087 MeV/nucleon Iron-56 beam used for radiobiology at the Alternating Gradient Synchrotron. Radiat. Res. 149, 560–569.
Zeitlin, C., Guetersloh, S.B., Heilbronn, L.H., Miller, J., 2006. Measurements of materials shielding properties with 1 GeV/nuc ^{56}Fe. Nucl. Instrum. Methods Phys. Res. B 252, 308–318.
Zeitlin, C., Fukumura, A., Guetersloh, S.B., Heilbronn, L.H., Iwata, Y., Miller, J., Murakami, T., 2007. Fragmentation cross sections of ^{28}Si at beam energies from 290A to 1200A MeV. Nucl. Phys. A 784, 341–367.